http://pubsonline.informs.org/journal/trsc/

TRANSPORTATION SCIENCE
Vol. 53, No. 2, March–April 2019, pp. 585–596
ISSN 0041-1655 (print), ISSN 1526-5447 (online)

Threshold Queueing to Describe the Fundamental Diagram of Uninterrupted Traffic

Niek Baer,[a] Richard J. Boucherie,[a] Jan-Kees C. W. van Ommeren[a]

[a] Stochastic Operations Research, Department of Applied Mathematics, University of Twente, 7500 AE Enschede, Netherlands

Contact: n.baer@utwente.nl (NB); r.j.boucherie@utwente.nl, https://orcid.org/0000-0002-1046-2044 (RJB); j.c.w.vanommeren@utwente.nl, https://orcid.org/0000-0002-0190-5085 (J-KCWvO)

Received: December 29, 2016
Revised: November 3, 2017
Accepted: February 23, 2018
Published Online in Articles in Advance: March 26, 2019

https://doi.org/10.1287/trsc.2018.0850

Abstract. Queueing because of congestion is an important aspect of road traffic. This paper provides a novel threshold queue that models the empirical shape of the fundamental diagram. In particular, we show that our threshold queue with two service phases captures the capacity drop that is eminent in the fundamental diagram of modern traffic. We use measurements on a Danish highway to illustrate that our threshold queue is indeed capable of capturing the fundamental diagram of real-world traffic systems. We furthermore indicate the modelling power of our threshold queue via a sensitivity study showing that our model is able to capture a wide range of shapes for the fundamental diagram.

Funding: This research is supported by the Centre for Telematics and Information Technology of the University of Twente.

Supplemental Material: The online appendix is available at https://doi.org/10.1287/trsc.2018.0850.

Keywords: threshold queue • hysteresis • capacity drop • fundamental diagram • matrix analytic methods • level-dependent quasi-birth-and-death process

1. Introduction

Greenshields (1935) captures the empirical relation between speed, flow and density for uninterrupted traffic in the fundamental diagram (see Figure 1). Mathematical models for uninterrupted traffic have been developed, and the fundamental diagram in its basic form is now well-understood (see, e.g., Newell (1993a, b, c) for a concise exposition).

Traffic jams are a major concern for highway operation and may occur in high-density traffic due to variability in driving speed. A wide range of traffic models has been developed over the past decades. These models are mainly from statistical physics and nonlinear dynamics (see Chowdhury et al. 2000, and Helbing 2001). Congestion because of variable arrival and/or service processes is the main topic of queueing theory that, however, has hardly been invoked to analyse the fundamental concepts of uninterrupted traffic flows. Notable exceptions are the models introduced by Heidemann (1996) and Jain and Smith (1997). However, with these models it seems not possible to capture the empirical shape of the fundamental diagram for modern traffic as shown in Figure 2 with the sharp drop in the density-flow diagram directly followed by a slowly decreasing part. This paper introduces a so-called threshold queue to model and capture the fundamental diagram.

Customers arrive to the threshold queue and require service from a server. Both the interarrival times and service times are controlled by a threshold policy consisting of a lower threshold L and an upper threshold U. The empty queue corresponds to a noncongested state in which the server has a high service speed. When the queue length exceeds U, the queue reaches a congested state in which the server switches to a low service speed. The queue will switch back to the noncongested state with high service rate once the queue length drops below L. Typically, $L < U$, which mimics the behaviour on highways where it takes some time for drivers to resume speed.

An important aspect of modern traffic flows is the *capacity drop*, the sharp descent in the fundamental diagram (see Figure 2). Helbing (2001) explains the capacity drop as the transition from noncongested traffic to congested traffic. When the density of vehicles reaches a certain critical value, ρ_2, traffic will become congested, and the average speed is significantly lower than in noncongested traffic. When density decreases and reaches another critical value, $\rho_1 \leq \rho_2$, a transition from congested traffic to noncongested traffic occurs, and traffic flows recover. In the density interval $[\rho_1, \rho_2]$, both congested and noncongested traffic flows exist, which indicates the existence of hysteresis. As is shown in our numerical results, it is precisely this hysteresis effect captured by the threshold queue that results in the capacity drop in the fundamental diagram of Figure 2 observed in empirical data for speed, flow, and density.

Figure 1. Fundamental Diagram from the Experimental Data of Greenshields

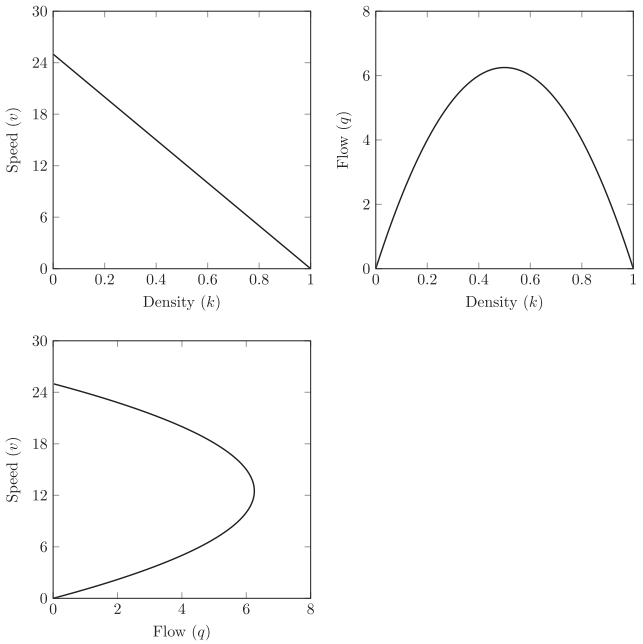

Source. Greenshields 1935.

Section 2 gives a brief overview of the literature on queueing models for uninterrupted traffic flows. The threshold queue model is introduced and analysed in Section 3. Results on the fundamental diagram obtained with the threshold queue are shown in Section 4. Section 5 gives concluding remarks.

2. Literature

Congestion is a key concept in queueing theory that models both the mesoscopic and macroscopic effects of randomness on delay and sojourn times. In interrupted traffic flows, where queues arise naturally at an intersection, queueing theory has been a popular tool since the early 1940s; see Boon (2011) for a recent survey. In uninterrupted traffic, however, queueing models have received far less attention in literature. In this section, we first focus on queueing models for uninterrupted traffic flows. These models also allow us to describe some key properties of the fundamental diagram. Starting from the literature surveys Ni (2013) and Wang et al. (2009, 2011), we provide an overview of the results on the fundamental diagram in Section 2.3.

2.1. Microscopic, Mesoscopic, and Macroscopic Models

Uninterrupted or highway traffic flow models can be characterised by their level of detail: microscopic, mesoscopic, and macroscopic.

In *microscopic models*, a high level of detail is used, in which each individual driver is characterised by its position and behaviour over time (Hoogendoorn and Bovy 2001, Ni 2011). In general, microscopic models lead to systems of (ordinary) differential equations (Helbing 2001). Well-known microscopic models are the car-following model (Chandler et al. 1958, Brackstone and McDonald 1999), the cellular automata model (Nagel 1996), and lane-changing models (Ahmed et al. 1996).

In *mesoscopic models*, the individual drivers are not distinguished (Hoogendoorn and Bovy 2001, Ni 2011). The behaviour of drivers is characterised in terms of the probability density $f(x, v, t)$ of vehicles at position x with speed v at time t. Examples of mesoscopic models are headway distribution models (Buckley 1968) and gas-kinetic continuum models (Prigogine and Andrews 1960, Prigogine and Herman 1971).

Macroscopic models have the lowest level of detail and consider only three variables for each position x and time t—average speed $v(x,t)$, traffic flow $q(x,t)$, and spatial vehicle density $k(x,t)$—that are related as $q(x,t) = v(x,t) \cdot k(x,t)$. These three variables are often presented in the fundamental diagram. Two classical examples of macroscopic models are the Lighthill–Whitham–Richards models (Lighthill and Whitham 1955a, b; Richards 1956) and the Payne models (Payne 1971).

For more elaborate surveys on traffic models for uninterrupted traffic flows, see Bellomo and Dogbe (2011), Helbing (2001), Hoogendoorn and Bovy (2001), Ni (2011), and van Woensel and Vandaele (2007).

Figure 2. (Color online) Fundamental Diagram from Experimental Data for Modern Traffic

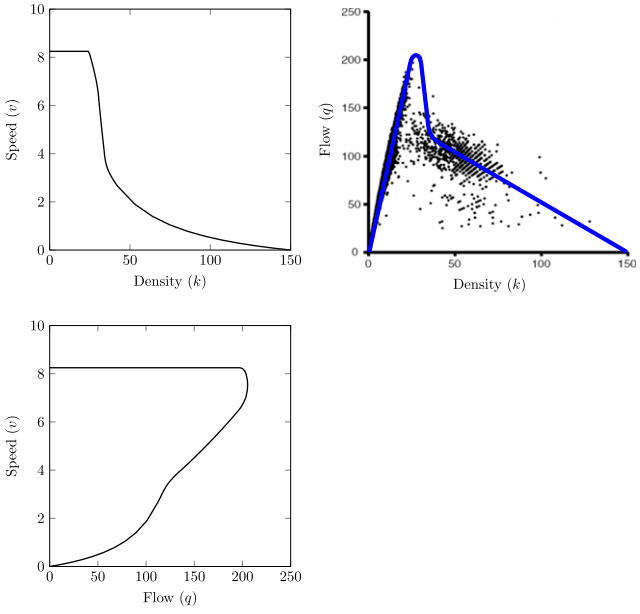

Source. Sugiyama et al. 2008.
Note. The flow-density diagram is fitted to the experimental data where q is the flow per 5 minutes, k is per km and v in km/5 min.

2.2. Queueing Theory in Uninterrupted Traffic Flows

Two main queueing theoretic approaches can be identified to model uninterrupted traffic: the queue with waiting room of Heidemann (1996) and the queue with blocking of Jain and Smith (1997). We use the following notation. Let k denote the traffic density, v the mean speed of a vehicle, q the flow rate, k_{jam} the jam or maximum density, and v_f the desired mean speed or free flow speed.

Heidemann's Model. Heidemann (1996) introduces an $M/G/1$ queueing system to model highway traffic. The server in the queueing system corresponds to a highway segment of length $1/k_{jam}$, which is the minimal part of the highway each vehicle requires. The mean service time in the queue is the average time it takes a vehicle in free-flow traffic to cross the segment: $\mathbb{E}[B] = 1/(k_{jam} \cdot v_f)$. The traffic density outside the chosen segment is k, so that the mean time between two arrivals is $\mathbb{E}[A] = 1/(k \cdot v_f)$. The probability of the server being busy is defined by

$$1 - \pi_0 = \frac{\mathbb{E}[B]}{\mathbb{E}[A]} = \frac{k}{k_{jam}}, \tag{1}$$

where π_0 denotes the probability of the queue being empty.

In the $M/G/1$ queue, an arriving vehicle may find the server busy upon arrival and must wait for service. The total time required to cross the segment is the sojourn time, $\mathbb{E}[S]$, which is the sum of the waiting time and the service time. For the $M/G/1$ queue the Pollaczek–Khintchine formula (Wolff 1989) gives

$$\mathbb{E}[S] = \mathbb{E}[B]\left[1 + \frac{\rho}{1-\rho} \cdot \frac{(1+c_s^2)}{2}\right],$$

where c_s is the coefficient of variation of the service time. The speed, v, of a vehicle passing the segment then is

$$v = \frac{1/k_{jam}}{\mathbb{E}[S]}. \tag{2}$$

Figure 3 gives the fundamental diagram for the $M/G/1$ queue for various choices of c_s.

Generalisations of Heidemann's model include the transient analysis of the $M/G/1$ queue (Heidemann 1999, 2001, 2002). Vandaele et al. (2000) and van Woensel (2003) consider the $G/G/s$ queue. Validation of their queueing model (van Woensel and Vandaele 2006, van Woensel et al. 2006) shows that the $M/G/1$ queue is a good model for noncongested traffic and that the $G/G/s$ is more suitable to model congested traffic. Accidents were incorporated by Baykal-Gürsoy et al. (2009) in an $M/MSP/c$ queue with service rates represented by a Markovian service process.

Jain and Smith's Model. An alternative approach to a queueing model for highway traffic is the $M/G/c/c$ model of Jain and Smith (1997), where an arrival that finds all servers occupied is blocked and cleared (lost). Their model is based on pedestrian flows in emergency evacuation planning (Yuhaski and Smith 1989). The servers correspond to a road segment. As the $M/G/c/c$ model does not incorporate waiting, the speed of a vehicle is obtained by the service time that equals the sojourn time in the queue. The capacity C of a road segment equals the number of vehicles that fit in this segment—that is, the product of the jam density, k_{jam}, the length of the road segment, L, and the number of lanes, N: $C = k_{jam} \cdot L \cdot N$. The mean speed of a vehicle, V_n, depends on the number of vehicles n on the road segment and is now a function that is input for the model. Two functions for V_n are considered (Yuhaski and Smith 1989, Jain and Smith 1997)

$$V_n = \frac{v_f}{C}(C + 1 - n),$$

that linearly decreases in the number of vehicles on the segment, and

$$V_n = v_f \cdot \exp\left[-\left(\frac{n-1}{\beta}\right)^{\gamma}\right],$$

for suitable constants γ and β (see Yuhaski and Smith 1989) that exponentially decreases with the number of vehicles. In Figure 4, we present the fundamental diagram obtained with the $M/G/c/c$ queue for both speed functions V_n.

A network of $M/G/c/c$ queues was considered by Cruz et al. (2005) and Cruz and Smith (2007). In this network, a blocked customer will occupy its server

Figure 3. Fundamental Diagram Obtained with Heidemann's $M/G/1$ Queue, $k_{jam} = 200/\text{km}$, $v_f = 120\,\text{km/h}$, and Varying Coefficient of Variation c_s

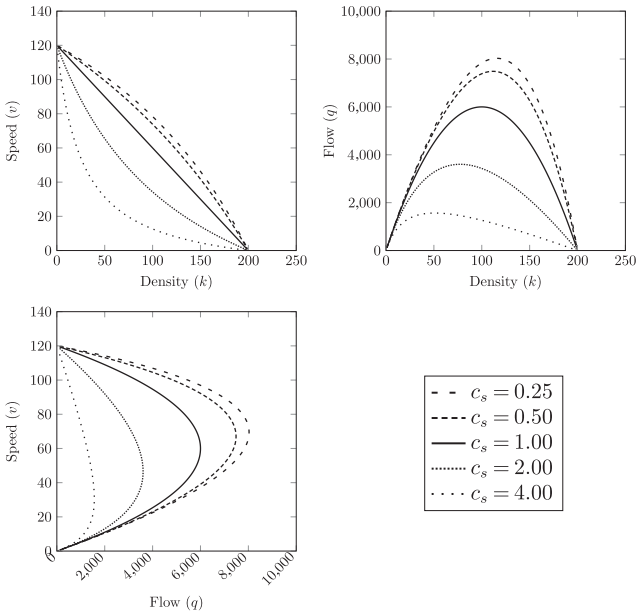

Figure 4. Fundamental Diagram Obtained with Jain and Smith's $M/G/c/c$ Queue for a Linear and Exponential Decreasing Speed, $k_{jam} = 200, v_f = 55$ mph

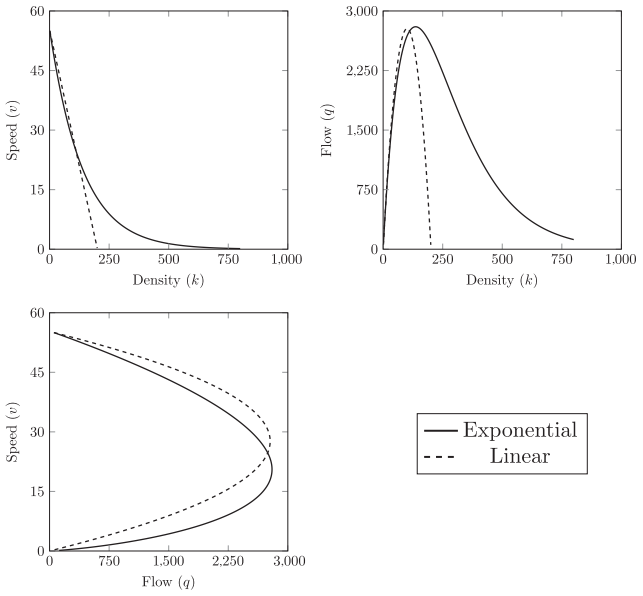

until it is no longer blocked. In Cruz et al. (2005) and Cruz and Smith (2007), simulation techniques and approximations were used to derive blocking probabilities, throughput, mean queue length, and mean waiting times.

Summary. The queueing models in literature result in a fundamental diagram similar to the fundamental diagram by Greenshields. However, these models do not capture the hysteresis effect as seen in modern traffic flows. The threshold queue in the next section mimics this hysteresis effect and will be shown to capture the resulting capacity drop.

2.3. Fundamental Diagram

The seminal work of Greenshields (1935) has initiated the research to find a simple formula capable of capturing the fundamental diagram of traffic flows. As can be seen in Figure 1, the fundamental diagram proposed by Greenshields has a linear speed–density relationship given by a single formula (see Table 1). The Greenshields model is an example of a single-regime traffic model. In multiregime traffic models, the speed–density relationship is a piecewise function, depending on the regime of the highway section—for instance, free-flow or congested (see Table 2). Below, we first consider single-regime models. Subsequently, we consider multiregime models.

For an overview of single-regime models that have been developed since Greenshields (1935), see Table 1 (adapted from Wang et al. 2009). In this table, we denote by v_c and k_c the speed and density at capacity—that is, when flow equals the maximum flow q_{max}. Furthermore, let ω_v denote the jam wave speed. Wang et al. (2009) fit several single regime models from Table 1 to empirical data. The Greenshields model describes a linear relationship between speed and density, causing a parabolic relationship between flow and density. Several models were introduced to better capture realistic traffic flows. The Greenberg (1959) model proposes a logarithmic speed–density relationship based on fluid-flow analogies. This logarithmic approach performs well under congested conditions ($v = 0$ when $k = k_{jam}$), but it does not satisfy boundary conditions at low densities ($v \to \infty$ as $k \to 0$). Underwood (1961) proposed an exponential speed–density relationship which obeys the boundary conditions at low densities but does not satisfy boundary conditions under congested conditions ($v \to 0$ for $k \to \infty$). This limitation is also found in the Northwestern model by Drake et al. (1967) in which a bell-shaped speed–density relationship was proposed. The Drew (1968) model and Pipes–Munjal model by Munjal and Pipes (1971) resemble the simple formulation of Greenshields with the introduction of an extra parameter n. This parameter n allows for extra degrees of freedom in fitting the models to empirical data. The general form of the Drew and Pipes–Munjal model is captured by the Kühne and

Table 1. Single Regime Speed–Density Relationships

Model	Function
Greenshields	$v = v_f\left(1 - \frac{k}{k_{jam}}\right)$,
Greenberg	$v = v_c \ln\left(\frac{k_{jam}}{k}\right)$,
Underwood	$v = v_f e^{-\frac{k}{k_c}}$,
Northwestern	$v = v_f e^{-\frac{1}{2}\left(\frac{k}{k_c}\right)^2}$,
Drew	$v = v_f\left(1 - \left(\frac{k}{k_{jam}}\right)^{n+\frac{1}{2}}\right)$,
Pipes-Munjal	$v = v_f\left(1 - \left(\frac{k}{k_{jam}}\right)^{n}\right)$,
Kühne and Rödiger	$v = v_f\left(1 - \left(\frac{k}{k_{jam}}\right)^{a}\right)^{b}$,
Modified Greenshields	$v = v_0 + (v_f - v_0)\left(1 - \frac{k}{k_{jam}}\right)^{n}$,
Newell	$v = v_f\left(1 - e^{-\frac{\lambda}{v_f}\left(\frac{1}{k} - \frac{1}{k_{jam}}\right)}\right)$,
Del Castillo and Benitez	$v = v_f\left(1 - e^{\frac{\lvert\omega_v\rvert}{v_f}\left(1 - \frac{k_{jam}}{k}\right)}\right)$,
Van Aerde	$k = \frac{1}{c_1 + \frac{c_2}{v_f - v} + c_3 v}$,
MacNicholas	$v = v_f\left(\frac{k_{jam}^n - k^n}{k_{jam}^n + ck^n}\right)$,
Wang	$v = v_0 + (v_f - v_0)\left(1 + e^{\frac{k - k_1}{\theta_1}}\right)^{-\theta_2}$.

Source. Adapted from Wang et al. (2009).

Table 2. Dual Regime Speed–Density Relationships

Model	Function
Edie	$v = \begin{cases} v_f e^{-\frac{k}{k_c}}, & k \le k_c, \\ c \ln\left(\frac{k_{jam}}{k}\right), & k > k_c. \end{cases}$
Triangular	$v = \begin{cases} v_f, & k \le k_{bp}, \\ \frac{v_f k_c}{k_c - k_{jam}}\left(1 - \frac{k_{jam}}{k}\right), & k > k_{bp}. \end{cases}$
Modified Greenshields	$v = \begin{cases} v_f, & k \le k_{bp}, \\ v_0 + (v_f - v_0)\left(\frac{k_{jam} - k}{k_{jam} - k_{bp}}\right)^{\alpha}, & k > k_{bp}. \end{cases}$
Modified Greenberg	$v = \begin{cases} v_f, & k \le k_{bp}, \\ c \ln\left(\frac{k_{jam}}{k}\right), & k > k_{bp}. \end{cases}$

Rödiger (1991) model. Recently, an extension was made to the Greenshields model by Mahmassani et al. (2009), creating the modified Greenshields model for single regime. In this model, which resembles both the Drew and Pipes–Munjal model, a parameter v_0 denoting the minimal speed at jam density was introduced, such that $v = v_0$ when $k = k_{jam}$. Based on generating functions, Del Castillo and Benitez (1995a, b) proposed a speed–density relationship based on the free flow speed v_f, jam density k_{jam}, and jam wave speed ω_v. The authors note that their model can also be obtained from Newell's car-following model in Newell (1961). The Van Aerde (1995) model was obtained from the Van Aerde car-following model and contains three extra parameters c_1, c_2, and c_3. These parameters can be obtained by solving the boundary conditions (see Rakha and Crowther 2002). A queueing theoretical background to the Van Aerde (1995) model is given in Wu and Rakha (2009), where a modified tandem server system is presented. The parameters of this queueing system, which are directly related to the parameters of the traffic model, can be estimated by field data. It is shown in MacNicholas (2008) that a model similar to the Van Aerde model can be obtained with fewer parameters. A comparison between the MacNicholas and Van Aerde model is made in MacNicholas (2008). Recently, Wang et al. (2011) proposed a logistic speed–density model based on five parameters. An important parameter in their model is k_t, the density at which the transition from free-flow to congested traffic occurs. The parameters θ_1 and θ_2 are used to fit the traffic model. For a more concise overview and visual comparison of a selection of the models in Table 1, see Ni (2013) and Wang et al. (2009).

In a multiregime traffic model, it is possible to use several single-regime models at the same time, one for each regime. This way, better fits could be obtained. A drawback of multiregime models lies in finding the point at which regimes change. Some multiregime models occurring in literature are listed in Table 2. Because any combination of single-regime models can serve as a multiregime model, this list is by no means extensive. The simplest multiregime traffic model is the Triangular model, named after the triangular shape of the flow-density plot, as used in Newell (1993b). The corresponding speed–density relationship is given by the piecewise functions in Table 2. Here, k_{bp} denotes the breakpoint density, the density at which the regime changes. Similar speed–density relationships are obtained with the modified Greenberg model (see Drake et al. 1967) and the modified Greenshields model (see Mahmassani et al. 2009). All three models describe a constant speed when $k \le k_{bp}$ after which the speed decreases to zero (or v_0). The multiregime model by Edie (1961) is a combination of the Underwood and Greenberg models. The Underwood model is used to describes traffic flows at low density ($k \le k_c$), and the Greenberg model is used to describe traffic flows during congestion ($k > k_c$). In Drake et al. (1967), two more multiregime models were introduced: one consisting of two regimes, whereas the other has three regimes. Both models assume a linear speed–density relation during the regimes, and both models were fitted to empirical data in Drake et al. (1967) and May (1990). In Wu (2002), a four0regime model is introduced where the four regimes are "free flow," "in convoy," "congested," and "jammed."

3. Threshold Queue with Hysteresis

In this section, we consider two basic queueing models that are used to describe the fundamental diagram. In the first subsection, we consider the $M/M/1$ queue with thresholds. As this model is too restrictive to describe the fundamental diagram satisfactorily, we also introduce the $PH/PH/1$ threshold queue. In Section 4, we numerically evaluate these models for certain settings.

3.1. The $M/M/1$ Threshold Queue

Consider a single server queue with finite buffer N where service rates are controlled by a threshold policy. Customers arrive according to a Poisson process with rate λ and require an exponential service time, depending on the stage of the queue. This stage is either noncongested (denoted by stage 1), with service rate μ_1 or congested (denoted by stage 2), with service rate μ_2 and is controlled by the threshold policy. Once an arrival occurs while the queue length is U, the stage changes from noncongested to congested. The stage changes back from congested to noncongested when the queue length is L and a departure occurs. The state space of this threshold queue is depicted in Figure 5. The stationary queue length probabilities π

Figure 5. State Diagram for the $M/M/1$ Threshold Queue with Finite Buffer

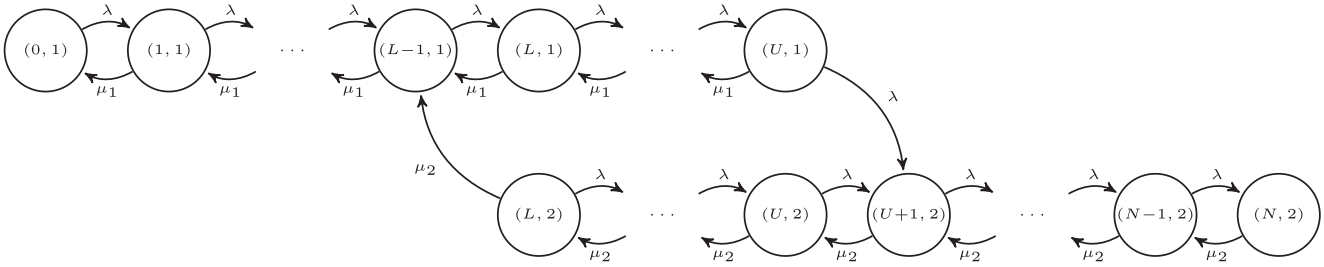

for this threshold queue can readily be obtained from standard Markov Chain analysis; see also Le Ny and Tuffin (2002). Let $\rho = \frac{\lambda}{\mu_1}$ and $\delta = \frac{\lambda}{\mu_2}$, then $\pi(i,1)$ and $\pi(i,2)$, where $\pi(i,j)$ denotes the probability of having i customers in the queue in stage j, are given by

$$\begin{aligned}
\pi(i,1) &= \pi(0,1)\rho^i, && i = 1,\dots,L-1,\\
\pi(i,1) &= \pi(0,1)\frac{\rho^i - \rho^{U+1}}{1-\rho^{U-L+2}}, && i = L,\dots,U,\\
\pi(i,2) &= \pi(0,1)\frac{\delta-\delta^{i-L+2}}{1-\delta}\,\frac{\rho^U-\rho^{U+1}}{1-\rho^{U-L+2}}, && i = L,\dots,U,\\
\pi(i,2) &= \pi(0,1)\frac{\delta^{i-U}-\delta^{i-L+2}}{1-\delta}\,\frac{\rho^U-\rho^{U+1}}{1-\rho^{U-L+2}}, && i = U+1,\dots,N,
\end{aligned} \tag{3}$$

with $\pi(0,1)$ such that

$$\left[\sum_{i=0}^{U}\pi(i,1) + \sum_{i=L}^{N}\pi(i,2)\right] = 1. \tag{4}$$

The mean sojourn time is then given by

$$\mathbb{E}[S] = \frac{1}{\Lambda}\left[\sum_{i=0}^{U} i\pi(i,1) + \sum_{i=L}^{N} i\pi(i,2)\right], \tag{5}$$

where Λ is the effective arrival rate to the queue:

$$\Lambda = \lambda\left[\sum_{i=0}^{U}\pi(i,1) + \sum_{i=L}^{N-1}\pi(i,2)\right].$$

Remark 1 (Infinite Buffer). Note that if we would consider a two-stage $M/M/1$ threshold queue with an infinite buffer, the stationary distribution in Equation (3) still holds, but with $\pi(0,1)$ such that

$$\left[\sum_{i=0}^{U}\pi(i,1) + \sum_{i=L}^{U}\pi(i,2) + \pi(U+1,2)\frac{1}{1-\delta}\right] = 1,$$

and mean sojourn time:

$$\mathbb{E}[S] = \frac{1}{\lambda}\left[\sum_{i=1}^{U} i\pi(i,1) + \sum_{i=L}^{U} i\pi(i,2) + \pi(U+1,2)\frac{N(1-\delta)+1}{(1-\delta^2)}\right],$$

and effective arrival rate

$$\Lambda = \lambda.$$

In order to use the threshold queue with a finite buffer as well as with an infinite buffer, we slightly altered Heidemann's method. Recall from Equations (1) and (2)

$$k = (1-\pi(0,1))k_{jam}, \qquad v = \frac{1/k_{jam}}{\mathbb{E}[S]}, \qquad q = k\cdot v. \tag{6}$$

For the threshold queue with an infinite buffer, we have that if $\lambda \to \mu_2$, that $\pi(0,1) \to 0$ and $k \to k_{jam}$. However, when the buffer size is finite $\pi(0,1) > 0$ for $\lambda \to \mu_2$. Therefore, we adjust Heidemann's method and define

$$k = (1-\pi(0,1))C, \qquad v = \frac{1/C}{\mathbb{E}[S]}, \qquad q = k\cdot v. \tag{7}$$

Here, we define $1/C$ to be the length of the highway segment that serves as the server, instead of $1/k_{jam}$ in Heidemann's method. The parameter C is obtained by fitting the model to empirical data. In this adjusted model we also define

$$k_{jam} = \lim_{\lambda\to\mu_2} k.$$

We may now obtain the capacity, q_{max}, critical density, k^*, and jam wave speed, ω_v, as follows. Let us denote by λ^* the value of λ, with $0 \le \lambda \le \mu_2$, for which the maximum flow, q_{max}, is obtained—that is, the value $\lambda = \lambda^*$ for which

$$\frac{d}{d\lambda}q = \left\{\frac{1}{\mathbb{E}[S]}\frac{d}{d\lambda}(1-\pi(0,1)) + (1-\pi(0,1))\frac{d}{d\lambda}\frac{1}{\mathbb{E}[S]}\right\} = 0.$$

From Equation (6), we now obtain

$$q_{max} = \frac{1-\pi(0,1)}{\mathbb{E}[S]}\bigg|_{\lambda=\lambda^*},$$
$$k^* = C(1-\pi(0,1))|_{\lambda=\lambda*},$$

where $|_{\lambda=\lambda*}$ indicates that we insert $\lambda = \lambda^*$ in these expressions.

Finally, we determine the jam wave speed, denoted by ω_v, as

$$\omega_v = \lim_{k\to k_{jam}} \frac{d}{dk} q = \lim_{\lambda\to\mu_2} \frac{\frac{d}{d\lambda} q}{\frac{d}{d\lambda} k}$$
$$= \lim_{\lambda\to\mu_2} \frac{\left\{\frac{1}{\mathbb{E}[S]}\frac{d}{d\lambda}(1-\pi(0,1)) + (1-\pi(0,1))\frac{d}{d\lambda}\frac{1}{\mathbb{E}[S]}\right\}}{C\frac{d}{d\lambda}(1-\pi(0,1))}.$$

The above expressions can readily be numerically evaluated for the $M/M/1$ threshold queue. In Section 4, we will fit our model to experimental data obtained for Danish highways, and we determine the capacity, critical density, and jam wave speed.

Remark 2 (Multilane traffic). Our model also captures multilane traffic. On a multilane highway, vehicles switch from high-density lanes to low-density lanes to improve their driving speed. To maintain safe driving distance, other vehicles decelerate, and the average speed decreases. Using the description by Helbing (2001) of the hysteretic transition from noncongested to congested traffic, we distinguish three density regions: light, medium, and heavy traffic. In light traffic ($k \le \rho_1$) vehicles will switch lanes, but they will not greatly affect other vehicles. In heavy traffic ($k \ge \rho_2$) vehicles will not be able to switch lanes due to high densities on all lanes. In medium traffic ($\rho_1 < k < \rho_2$) vehicles will switch lanes, causing average speed to decrease and density to increase. Once the density reaches ρ_2, the system becomes congested, and the average speed is considerably lower than in noncongested traffic. When we aggregate all lanes, the hysteresis in this multilane system resembles that in our single server threshold queue.

3.2. The *PH*/*PH*/1 Threshold Queue

For traffic modelling, the assumption of Poisson arrivals and exponential service is far from realistic. Therefore, we consider the $PH/PH/1$ threshold queue below in which both the interarrival times and service times are of phase type. The phase-type distribution allows us to approximate any distribution with nonnegative support arbitrarily close (see Hordijk and Schassberger 1982). We refer to the online appendix for a detailed description of the procedure described in this section.

Consider the $PH/PH/1$ threshold queue with interarrival times and service times having phase-type (PH) distribution. In the $PH/PH/1$ threshold queue the interarrival times are $PH(\boldsymbol{\Lambda}, \boldsymbol{\lambda})$ distributed and the service times are either $PH(\boldsymbol{M}_1, \boldsymbol{\mu}_1)$ (noncongested) or $PH(\boldsymbol{M}_2, \boldsymbol{\mu}_2)$ (congested) distributed. We assume that the queue is stable, as the mean service time in the congested stage is less than the mean interarrival time. Furthermore, we assume that the mean service time in the congested stage is larger than the mean service time in the noncongested stage.

We model the $PH/PH/1$ threshold queue as a level-dependent quasi-birth-and-death (LDQBD) process. The generator $\boldsymbol{Q}$ of this LDQBD has the following tridiagonal structure:

$$\boldsymbol{Q} = \begin{bmatrix} \boldsymbol{L}^{(0)} & \boldsymbol{F}^{(0)} & 0 & \cdots & & \\ \boldsymbol{B}^{(1)} & \boldsymbol{L}^{(1)} & \boldsymbol{F}^{(1)} & \ddots & & \\ 0 & \boldsymbol{B}^{(2)} & \boldsymbol{L}^{(2)} & \ddots & & \\ \vdots & \ddots & \ddots & \ddots & \boldsymbol{F}^{(i-1)} & \\ & & & \boldsymbol{B}^{(i)} & \boldsymbol{L}^{(i)} & \ddots \\ & & & & \ddots & \ddots \end{bmatrix}.$$

Here, $\boldsymbol{F}^{(i)}$ describes the *forward* transitions from level i to level $i+1$ (arrivals), $\boldsymbol{L}^{(i)}$ the *local* transition within level i and $\boldsymbol{B}^{(i)}$ the *backward* transitions from level i to level $i-1$ (departures).

Let $\boldsymbol{\pi} = [\boldsymbol{\pi}_0, \boldsymbol{\pi}_1, \dots]$ denote the probability vector such that $\boldsymbol{\pi Q} = \boldsymbol{0}$ and $\boldsymbol{\pi e} = 1$ with $\boldsymbol{e}^{(i)}$ a vector of all ones. The elements of the probability vector $\boldsymbol{\pi}_i$ describe the probability of being in a certain phase and in level i—that is, the probability of having i customers in the queue. If the LDQBD is irreducible, aperiodic and positive recurrent, the stationary queue length distribution $\boldsymbol{\pi}$ is given by

$$\boldsymbol{\pi}_i = \boldsymbol{\pi}_0 \prod_{n=0}^{i-1} \boldsymbol{R}^{(n)}, \quad i = 1, 2, \dots,$$

where $\boldsymbol{\pi}_0$ is subject to the boundary conditions

$$\boldsymbol{\pi}_0(\boldsymbol{L}^{(0)} + \boldsymbol{R}^{(0)}\boldsymbol{B}^{(1)}) = \boldsymbol{0},$$

and to the normalisation conditions

$$\boldsymbol{\pi}_0\left(\sum_{i=0}^{\infty}\prod_{n=0}^{i-1}\boldsymbol{R}^{(n)}\right)\boldsymbol{e} = 1,$$

where the empty product is, by convention, the identity matrix of suitable size. The matrices $\boldsymbol{R}^{(n)}$ are the minimal nonnegative solution (Bright and Taylor 1995) to the set of equations

$$\boldsymbol{F}^{(n)} + \boldsymbol{R}^{(n)}\boldsymbol{L}^{(n+1)} + \boldsymbol{R}^{(n)}\boldsymbol{R}^{(n+1)}\boldsymbol{B}^{(n+2)} = \boldsymbol{0}, \quad n = 0, 1, \dots$$

Let $\mathbb{E}[A]$ denote the mean interarrival time and $\mathbb{E}[S]$ the mean sojourn time. We compute the mean queue length using $\boldsymbol{\pi}$ and determine the mean sojourn time using Little's Law:

$$\mathbb{E}[S] = \mathbb{E}[A]\left[\sum_{n=0}^{\infty} n\boldsymbol{\pi}_n\boldsymbol{e}\right].$$

4. Numerical Analysis

In this section, we numerically investigate the fundamental diagram given by the threshold queues. First, we consider the validity of threshold queueing to model highway traffic. To this end, we will restrict ourselves to the $M/M/1$ case, as this captures the qualitative behaviour without the fine-tuning quantitative option of the $PH/PH/1$ queue. Then, we investigate the additional modelling power of the $PH/PH/1$ queue. To this end, we perform a sensitivity analysis on the influence of the parameters L, U, μ_1 and μ_2 in the $M/M/1$ threshold queue on the shape of the fundamental diagram and on the distribution functions in the $PH/PH/1$ threshold queue (while leaving L, U, μ_1 and μ_2 unchanged). The advantage of using the $PH/PH/1$ queue compared with $M/M/1$ queue is that many more types of fundamental diagrams can be generated by changing the parameters. However, fitting the five parameters of the $M/M/1$ queue to empirical data are much easier than fitting the many parameters of the $PH/PH/1$ queue.

4.1. Model Validation

In Figure 6, the $M/M/1$ threshold queue is fitted to empirical data points obtained from measurements made in September and October 2013 on three different locations on the Helsingørmotorvejen (two-lane) in Denmark made available by DTU Transport, Denmark (Prameswari and Giacomo Prato 2013). DTU Transport provided us three data sets with measurement on difference time intervals: hourly measurements near Hørsholm, 15-minute measurements near Sandbjerg, and 5-minute measurements near Kokkedal. These data sets were uniformised to represent hourly measurements on all three locations. The data points in Figure 6(a) refer to the measurements near Hørsholm; the data points in Figure 6(b) refer to the measurements near Sandbjerg, and the data points in Figure 6(c) refer to the measurements near Kokkedal. The curves in each subfigure show the best fit using the $M/M/1$ threshold queue for three different buffer sizes, $N = 10$, $N = 20$, and $N = \infty$. The parameters for these curves, as well as the jam density, k_{jam}, the capacity, q_{max}, critical density, k^*, and jam wave speed, ω_v, are given in Table 3. We show that the qualitative behaviour of the M/M/1 threshold queue captures the behaviour of the fundamental diagram of highway traffic.

Figure 6 and Table 3 show that both the jam density, k_{jam}, and jam wave speed, ω_v, can be regulated by the buffer size N. Decreasing the buffer size results in a decreasing jam density and decreasing jam wave speed.

4.2. Sensitivity of Fundamental Diagram for the *M/M/1* Threshold Queue

Figure 7 characterises the fundamental diagram of the $M/M/1$ threshold queue for four different scenarios. Each scenario is based on the basic scenario, with $k_{jam} = 1, \mu_1 = 25, \mu_2 = 15, L = 15$ and $U = 10$, but one of the four parameters is altered: (1) the lower threshold, L, (2) the upper threshold, U, (3) the high service rate, μ_1, and (4) the low service rate, μ_2. k_{jam} is kept unchanged because it is merely a scaling constant. This parameter setting is chosen to clearly illustrate how these parameters influence the fundamental diagram.

The effects of altering L are minimal, as can be seen in Figure 7(a). Figure 7(b) shows that the steepness of the capacity drop increases by increasing U. Figure 7, (c) and (d) show that the position of the capacity drop varies with μ_1 or μ_2 and that flows increase with μ_1.

4.3. Sensitivity of Fundamental Diagram for the *PH/PH/1* Threshold Queue

Figure 8 characterises the fundamental diagram of the $PH/PH/1$ threshold queue for four different scenarios.

Figure 6. Flow-Density Diagram Obtained with a Fitted $M/M/1$ Threshold Queue

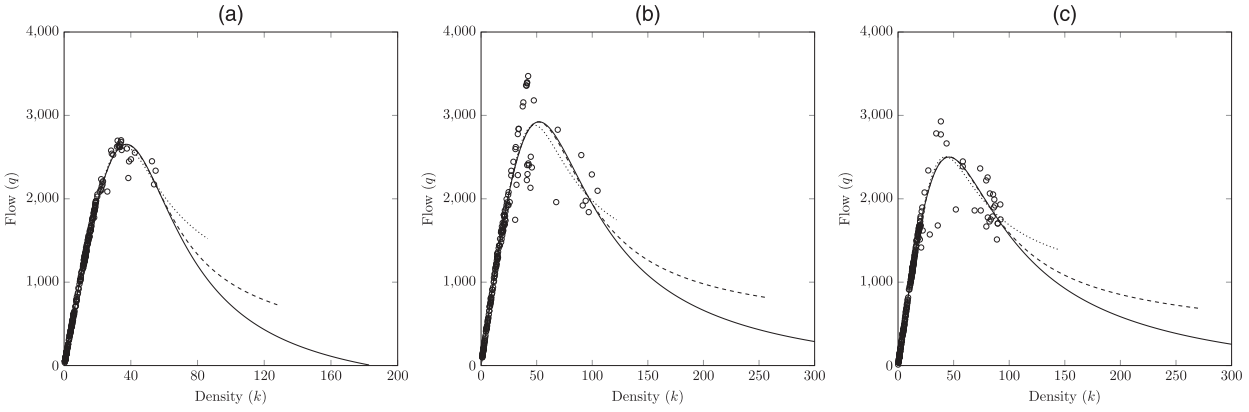

Note. The flow-density curve was fitted to empirical flow-density points of a Danish motorway with $N = 10$(.....), $N = 20$(—) and $N = \infty$(—).

Table 3. Parameters for the Three $M/M/1$ Threshold Queues in Figure 6

	(a) Hørsholm			(b) Sandbjerg			(c) Kokkedal		
N	10	20	∞	10	20	∞	10	20	∞
L	1	1	1	2	2	2	1	1	1
U	3	3	3	2	2	2	2	2	2
μ_1	26,190.13	21,301.42	20,984.62	103,728.36	55,584.00	51,689.51	86,078.55	50,447.65	47,969.29
μ_2	5,896.21	6,899.43	6,970.39	6,160.00	7,605.49	7,775.93	5,719.23	6,701.10	6,782.52
C	234.80	187.81	184.75	1146.85	598.78	554.46	938.01	538.23	510.46
k_{jam}	86.34	128.25	184.75	122.24	259.07	554.46	144.16	271.82	510.46
q_{max}	2,635.07	2,652.65	2,653.70	2,882.80	2,922.13	2,923.28	2,503.89	2,504.77	2,500.60
k^*	35.83	37.20	37.36	48.08	51.61	52.19	42.83	45.59	45.89
ω_v	−14.18	−9.17	−3.37	−8.38	−2.30	−0.53	−4.49	−1.95	−0.65

We select phase-type distributions such that the mean interarrival times and mean service times (in both stages) are the same as in the $M/M/1$ threshold queue of Figure 6. We consider three different distributions: the hyperexponential distribution with four phases, H_4; the exponential distribution, M; and the Erlang distribution with four phases, E_4, with respectively $c^2_{H_4}=1.5744$, $c^2_M=1$, and $c^2_{E_4}=0.25$. Furthermore, we set $L=5$ and $U=15$.

In Figure 8(a), we vary $PH(\boldsymbol{M}_2, \boldsymbol{\mu}_2)$, the distribution of the congested service process. We set $PH(\boldsymbol{\Lambda}, \boldsymbol{\lambda}) = H_4$ and $PH(\boldsymbol{M}_1, \boldsymbol{\mu}_1) = H_4$. It can be seen that the fundamental diagrams for the three different distributions of $PH(\boldsymbol{M}_2, \boldsymbol{\mu}_2)$ are similar. This implies that the coefficient of variation of $PH(\boldsymbol{M}_2, \boldsymbol{\mu}_2)$ has minor influence on the fundamental diagram.

Figure 7. Flow-Density Diagram for the $M/M/1$ Threshold Queue for Several L (a), U (b), μ_1 (c), and μ_2 (d)

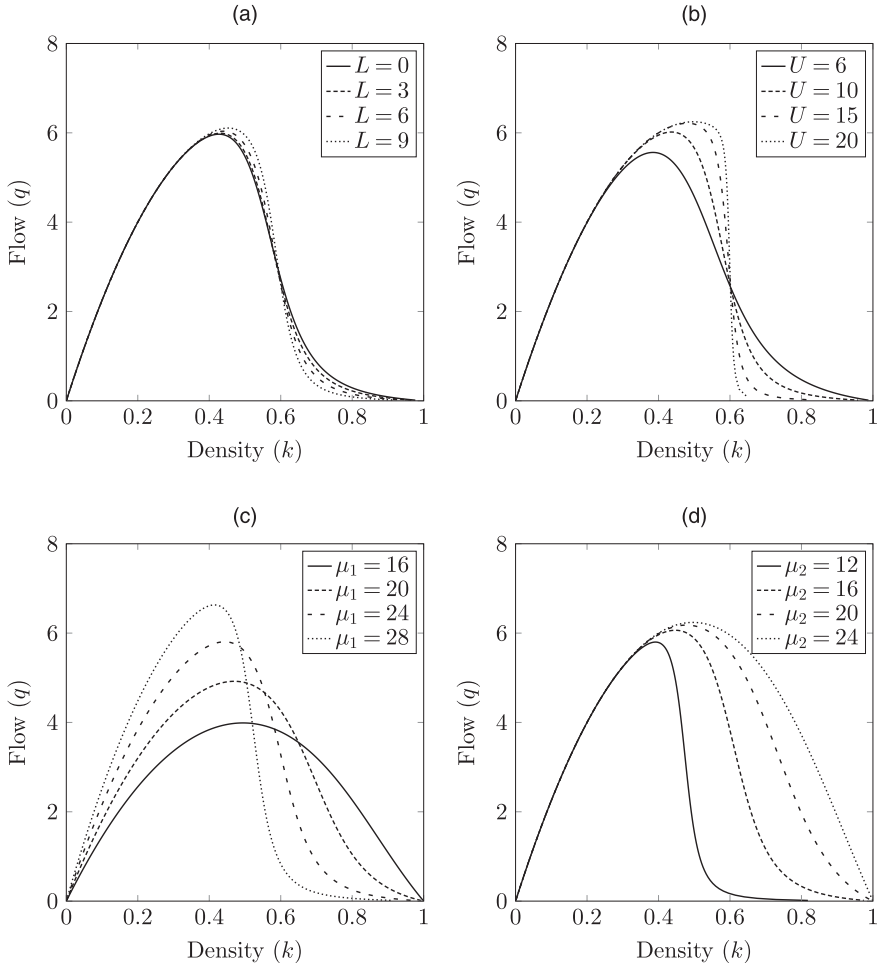

Figure 8. Flow-Density Diagram for the $PH/PH/1$ Threshold Queue for Various Distributions for the Congested Service Process (a), the Arrival Process (b), and the Noncongested Service Process (c and d)

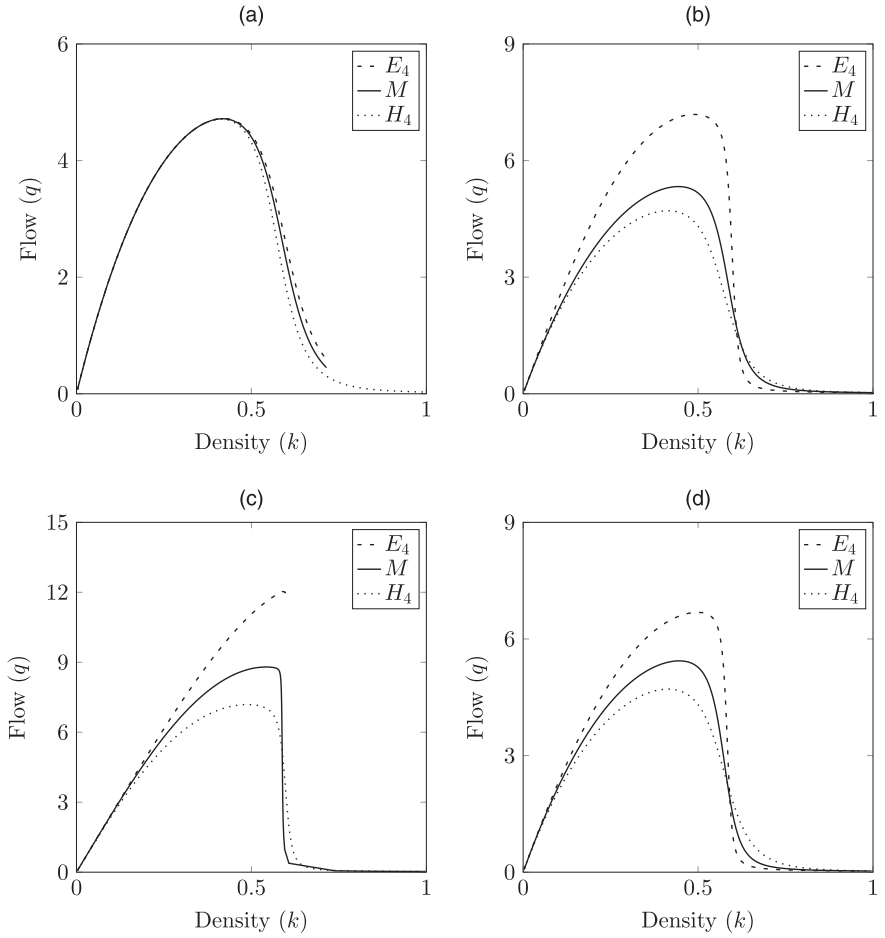

In Figure 8(b), we vary $PH(\boldsymbol{\Lambda}, \boldsymbol{\lambda})$, the distribution of the arrival process. We set $PH(\boldsymbol{M}_1, \boldsymbol{\mu}_1) = H_4$ and $PH(\boldsymbol{M}_2, \boldsymbol{\mu}_2) = H_4$. We observe that increasing variability in the arrival process reduces speed and flow for density $k < 0.6$. For $k > 0.6$, flows and speeds increase when the variability decreases.

In Figure 8(c), we vary $PH(\boldsymbol{M}_1, \boldsymbol{\mu}_1)$, the distribution of the noncongested service process. We set $PH(\boldsymbol{M}_1, \boldsymbol{\mu}_1) = H_4$ and $PH(\boldsymbol{\Lambda}, \boldsymbol{\lambda}) = E_4$. Here, the effects of the Erlang distribution are clearly visible in the fundamental diagram. In the case where both the arrival process and the noncongested service process are Erlang with four phases, the fundamental diagram reaches a maximum density of 0.6. This is a result of the low probability of reaching the congested stage caused by the low variability in the E_4 distribution. Note that for deterministic arrival and service processes, the congested stage is never reached. The maximum density of 0.6 is obtained for a mean interarrival time close to $1/15$, the mean service time in the congested stage. For this value, the queue is still stable, and the density is $15/25 = 0.6$.

In Figure 8(d), we vary $PH(\boldsymbol{M}_1, \boldsymbol{\mu}_1)$, the distribution of the noncongested service process. We set $PH(\boldsymbol{M}_1, \boldsymbol{\mu}_1) = H_4$ and $PH(\boldsymbol{\Lambda}, \boldsymbol{\lambda}) = H_4$. The results are similar to those for Figure 8(b). Increasing variability of the noncongested service process decreases flow and speeds for $k < 0.6$. For $k > 0.6$, flows and speeds increase when the variability decreases.

5. Conclusions

This paper has introduced the $PH/PH/1$ threshold queue to study the parameters of traffic that influence the shape of the fundamental diagram, including the capacity drop in this diagram observed in empirical data for modern traffic flows.

The $PH/PH/1$ threshold queue has two service regimes—high and low service rates—and switches from high rates to low rates when the queue length exceeds the upper threshold and returns to high rates when the queue length falls below the lower threshold, where the lower threshold is smaller than the upper threshold.

The $M/M/1$ threshold queue was successfully fitted to experimental data, and the jam density, capacity,

critical density, and jam wave speed were computed for different data sets.

Sensitivity analysis revealed that steepness of the capacity drop and traffic density where it occurs are determined by, respectively, the value of the higher threshold and the mean service times.

The service distribution in the congested stage has minor influence on the fundamental diagram. In contrast, increasing variability in the arrival process or noncongested service process is shown to reduce both speed and flow for a density less than the capacity drop density.

With the two models for traffic that we introduce in this paper, we can describe the fundamental diagram for a single road segment very well. To look at the behaviour of a network of traffic segments, we need another model because the arrival process to a downstream segment depends on the stages of the upstream segments. We can then model this whole system by an LDQBD, keeping track of the stage of every link; however, here the number of phases in a level will be too large to give a tractable model. As a consequence, approximative models need to be developed.

Acknowledgments

The authors acknowledge DTU Denmark for sharing the highway traffic data used to validate the authors' model.

References

Ahmed K, Ben-Akiva M, Koutsopoulos H, Mishalani R (1996) Models of freeway lane changing and gap acceptance behavior. Lesort J-B, ed. *Proc. 13th Internat. Sympos. Transportation Traffic Theory* (Pergamon, Oxford, UK), 501–515.

Baykal-Gürsoy M, Xiao W, Ozbay K (2009) Modeling traffic flow interrupted by incidents. *Eur. J. Oper. Res.* 195(1):127–138.

Bellomo N, Dogbe C (2011) On the modeling of traffic and crowds: A survey of models, speculations, and perspectives. *SIAM Rev.* 53(3):409–463.

Boon M (2011) Polling models—From theory to traffic intersections. Unpublished PhD thesis, Eindhoven University of Technology, Eindhoven, Netherlands.

Brackstone M, McDonald M (1999) Car-following: A historical review. *Transportation Res. Part F: Traffic Psych. Behav.* 2(4): 181–196.

Bright L, Taylor P (1995) Calculating the equilibrium distribution in level dependent quasi-birth-and-death processes. *Comm. Statist. Stochastic Models* 11(3):497–525.

Buckley D (1968) A semi-Poisson model of traffic flow. *Transportation Sci.* 2(2):107–133.

Chandler R, Herman R, Montroll E (1958) Traffic dynamics: Studies in car following. *Oper. Res.* 6(2):165–184.

Chowdhury D, Santen L, Schadschneider A (2000) Statistical physics of vehicular traffic and some related systems. *Phys. Rep.* 329(4–6): 199–329.

Cruz F, Smith J (2007) Approximate analysis of $M/G/c/c$ state-dependent queueing networks. *Comput. Oper. Res.* 34(8):2332–2344.

Cruz F, Smith J, Medeiros R (2005) An $M/G/c/c$ state-dependent network simulation model. *Comput. Oper. Res.* 32(4):919–941.

Del Castillo J, Benitez F (1995a) On the functional form of the speed-density relationship I: General theory. *Transportation Res. Part B: Methodological* 29(5):373–389.

Del Castillo J, Benitez F (1995b) On the functional form of the speed-density relationship II: Empirical investigation. *Transportation Res. Part B: Methodological* 29(5):391–406.

Drake J, Schofer J, May A (1967) A statistical analysis of speed-density hypotheses. *Highway Res. Record* (154):53–87.

Drew D (1968) *Traffic Flow Theory and Control* (McGraw-Hill, New York).

Edie J (1961) Car-following and steady-state theory for noncongested traffic. *Oper. Res.* 9(1):66–76.

Greenberg H (1959) An analysis of traffic flow. *Oper. Res.* 7(1):79–85.

Greenshields B (1935) A study of traffic capacity. *Proc. 14th Annual Meeting Highway Res. Board* (Highway Research Board, Washington, DC), 448–477.

Heidemann D (1996) A queueing theory approach to speed-flow-density relationships. Lesort J-B, ed. *Proc. 13th Internat. Sympos. Transportation Traffic Theory* (Pergamon, Oxford, UK), 103–118.

Heidemann D (1999) Non-stationary traffic flow from a queueing theory viewpoint. Ceder A, ed. *Proc. 14th Internat. Sympos. Transportation Traffic Theory* (Pergamon, Oxford, UK).

Heidemann D (2001) A queueing theory model of nonstationary traffic flow. *Transportation Sci.* 35(4):405–412.

Heidemann D (2002) Mathematical analysis of non-stationary queues in traffic flow with particular consideration of the coordinate transformation technique. Taylor MAP, ed. *Transportation and Traffic Theory in the 21st Century* (Emerald, Bingley, UK), 675–695.

Helbing D (2001) Traffic and related self-driven many-particle systems. *Rev. Modern Phys.* 73(4):1067–1141.

Hoogendoorn S, Bovy P (2001) State-of-the-art of vehicular traffic modeling. *J. Systems Control Engrg.* 215(4):283–303.

Hordijk A, Schassberger R (1982) Weak convergence for generalized semi-Markov processes. *Stochastic Processes Their Appl.* 12(3): 271–291.

Jain R, Smith J (1997) Modeling vehicular traffic flow using $M/G/c/c$ state dependent queueing models. *Transportation Sci.* 31(4):324–336.

Kühne R, Rödiger M (1991) Macroscopic simulation model for freeway traffic with jams and stop-start waves. Nelson BL, Kelton WK, Clark GM, eds. *Proc. 1991 Winter Simulation Conf.* (IEEE, New York), 762–770.

Le Ny L, Tuffin B (2002) A simple analysis of heterogeneous multi-server threshold queues with hysteresis. *Proc. Appl. Telecomm. Sympos., San Diego*.

Lighthill M, Whitham G (1955a) On kinematic waves. I. Flood movement in long rivers. *Proc. Roy. Soc. London Part A* 229(1178): 281–316.

Lighthill M, Whitham G (1955b) On kinematic waves. II. A theory of traffic flow on long crowded roads. *Proc. Roy. Soc. London Part A* 229(1178):317–345.

MacNicholas M (2008) A simple and pragmatic representation of traffic flow. *Proc. Sympos. Fundamental Diagram: 75 Years* (Transportation Research Board, Washington, DC), 161–177.

Mahmassani H, Dong J, Kim J, Chen R, Park B (2009) Incorporating weather impacts in traffic estimation and prediction systems. Technical Report FHWA-JPO-09-065, U.S. Department of Transportation, Washington, DC.

May A (1990) *Traffic Flow Fundamentals* (Prentice-Hall, Inc., Englewood Cliffs, NJ).

Munjal P, Pipes L (1971) Propagation of on-ramp density perturbations on uni-directional and two- and three-lane freeways. *Transportation Res.* 5(4):241–255.

Nagel K (1996) Particle hopping models and traffic flow theory. *Phys. Rev. E* 53(5):4655–4672.

Newell G (1961) Nonlinear effects in the dynamics of car following. *Operation Res.* 9(2):209–229.

Newell G (1993a) A simplified theory of kinematic waves in highway traffic, part I: General theory. *Transportation Res. Part B: Methodological* 27(4):281–287.

Newell G (1993b) A simplified theory of kinematic waves in highway traffic, part II: Queueing at freeway bottlenecks. *Transportation Res. Part B: Methodological* 27(4):289–303.

Newell G (1993c) A simplified theory of kinematic waves in highway traffic, part III: Multi-destination flows. *Transportation Res. Part B: Methodological* 27(4):305–313.

Ni D (2011) Multiscale modeling of traffic flow. *Math. Aeterna* 1(1): 27–54.

Ni D (2013) A unified perspective on traffic flow theory, part II: The unified diagram. *Appl. Math. Sci.* 7(40):1947–1963.

Payne H (1971) Models of freeway traffic and control. *Mathematical Models of Public Systems* (Simulation Councils, Inc., San Diego).

Prameswari N, Giacomo Prato C (2013) DTU Denmark. Data provided via personal communication with the authors, September–December.

Prigogine I, Andrews F (1960) A Boltzmann-like approach for traffic flow. *Oper. Res.* 8(6):789–797.

Prigogine I, Herman R (1971) *Kinetic Theory of Vehicular Traffic* (American Elsevier, New York).

Rakha H, Crowther B (2002) Comparison of Greenshields, Pipes, and Van Aerde car-following and traffic stream models. *Transportation Res. Record: J. Transportation Res. Board* 1802(1):248–262.

Richards P (1956) Shock waves on the highway. *Oper. Res.* 4(1):42–51.

Sugiyama Y, Fukui M, Kikuchi M, Hasebe K, Nakayama A, Nishinari K, Tadaki S, Yukawa S (2008) Traffic jams without bottlenecks—Experimental evidence for the physical mechanism of the formation of a jam. *New J. Phys.* 10(3):033001.

Underwood R (1961) *Speed, Volume, and Density Relationship: Quality and Theory of Traffic Flow* (Bureau of Highway Traffic, University Park, PA), 141–188.

Van Aerde M (1995) Single regime speed-flow-density relationship for congested and uncongested highways. *Proc. 74th Annual Meeting Transportation Res. Board* (Transportation Research Board, Washington, DC).

van Woensel T (2003) Models for uninterrupted traffic flows—A queueing approach. PhD thesis, Universiteit Antwerpen, Antwerpen, Belgium.

van Woensel T, Vandaele N (2006) Empirical validation of a queueing approach to uninterrupted traffic flows. *4OR* 4(1):59–72.

van Woensel T, Vandaele N (2007) Modeling traffic flows with queueing models: A review. *Asia Pacific J. Oper. Res.* 24(4):435–461.

van Woensel T, Wuyts B, Vandaele N (2006) Validating state-dependent queueing models for uninterrupted traffic flows using simulation. *4OR* 4(2):159–174.

Vandaele N, van Woensel T, Verbruggen A (2000) A queueing based traffic flow model. *Transportation Res. Part D: Transport Environment* 5(2):121–135.

Wang H, Li J, Chen Q, Ni D (2009) Speed-density relationship: From deterministic to stochastic. *Proc. 88th Annual Meeting Transportation Res. Board* (Transportation Research Board, Washington, DC).

Wang H, Li J, Chen Q, Ni D (2011) Logistic modeling of the equilibrium speed-density relationship. *Transportation Res. Part A: Policy Practice* 45(6):554–566.

Wolff R (1989) *Stochastic Modelling and the Theory of Queues* (Prentice-Hall, Englewood Cliffs, NJ).

Wu N (2002) A new approach for modeling of fundamental diagrams and its applications. *Transportation Res. Part A: Policy Practice* 36(10):867–884.

Wu N, Rakha H (2009) Derivation of the Van Aerde traffic stream model from tandem-queueing theory. *Transportation Res. Record: J. Transportation Res. Board* 2124(1):18–27.

Yuhaski S Jr, Smith J (1989) Modeling circulation systems in buildings using state dependent queueing models. *Queueing Systems* 4(4): 319–338.